Monthly Notices
of the
ROYAL ASTRONOMICAL SOCIETY

Mon. Not. R. Astron. Soc. **419,** 1376–1389 (2012) doi:10.1111/j.1365-2966.2011.19793.x

The chemical evolution of globular clusters – II. Metals and fluorine

P. Sánchez-Blázquez,[1⋆] A. Marcolini,[2] B. K. Gibson,[2,3,4] A. I. Karakas,[5] K. Pilkington[2,3,4] and F. Calura[2]

[1]*Departamento de Física Teórica, Universidad Autónoma de Madrid, E28049, Cantoblanco, Madrid, Spain*
[2]*Jeremiah Horrocks Institute, University of Central Lancashire, Preston PR1 2HE*
[3]*Department of Astronomy and Physics, St Mary's University, Halifax, Nova Scotia, B3H 3C3, Canada*
[4]*Monash Centre for Astrophysics, School of Mathematical Sciences, Monash University, Clayton, VIC 3800, Australia*
[5]*Research School of Astronomy and Astrophysics, Mt Stromlo Observatory, Weston Creek, ACT 2611, Australia*

Accepted 2011 September 9. Received 2011 September 6; in original form 2011 March 16

ABSTRACT

In the first paper of this series, we proposed a new framework in which to model the chemical evolution of globular clusters. This model is predicated upon the assumption that clusters form within an interstellar medium enriched locally by the ejecta of a single Type Ia supernova and varying numbers of asymptotic giant branch stars, superimposed on an ambient medium pre-enriched by low-metallicity Type II supernovae. Paper I was concerned with the application of this model to the observed abundances of several reactive elements and so-called non-metals for three classical intermediate-metallicity clusters, with the hallmark of the work being the successful recovery of many of their well-known elemental and isotopic abundance anomalies. Here, we expand upon our initial analysis by (i) applying the model to a much broader range of metallicities (from the factor of 3 explored in Paper I, to now a factor of ∼50; i.e. essentially, the full range of Galactic globular cluster abundances; and (ii) incorporating a broader suite of chemical species, including a number of iron-peak isotopes, heavier α-elements and fluorine. While allowing for an appropriate fine-tuning of the model input parameters, most empirical globular cluster abundance trends are reproduced; our model would suggest the need for a higher production of calcium, silicon and copper in low-metallicity (or so-called 'prompt') Type Ia supernovae than predicted in current stellar models in order to reproduce the observed trends in NGC 6752, and a factor of 2 reduction in carbon production from asymptotic giant branch stars to explain the observed trends between carbon and nitrogen. Observations of heavy-element isotopes produced primarily by Type Ia supernovae, including those of titanium, iron and nickel, could support/refute unequivocally our proposed framework, although currently the feasibility of the proposed observations is well beyond current instrumental capabilities. Hydrodynamical simulations would be necessary to study its viability from a dynamical point of view.

Key words: stars: abundances – stars: AGB and post-AGB – stars: chemically peculiar – globular clusters: general.

1 INTRODUCTION

Globular clusters (GCs) are gravitationally bound systems containing hundreds of thousands of stars, each cluster orbiting about a parent galaxy. The Milky Way (MW) itself has more than 150 associated GCs (Harris 1996). While conceptually simple, internally coeval systems from a chemical perspective, GCs are extremely interesting in the sense that they show a large variation in the abundances of light elements (i.e. Li, C, N, O, F, Na, Mg and Al) (e.g. Smith 1987; Kraft et al. 1993; Cohen, Briley & Stetson 2002; Grundahl et al. 2002; Yong et al. 2003; Sneden et al. 2004; Cohen & Meléndez 2005; Pasquini et al. 2005; Smith et al. 2005; Yong et al. 2005; Carretta et al. 2006; Bonifacio et al. 2007; Gratton et al. 2007; Marino et al. 2008, and references therein) both internally to a given cluster and between clusters. Conversely, the abundances of heavier α (e.g. Si, Ca and Ti), iron-peak (e.g. Fe, Ni and Cu) and neutron-capture elements (e.g. Ba, La and Eu) do not, in general, show the same star-to-star variation.

Correlated (and anti-correlated) elemental and isotopic (anomalous) trends between these various nuclei are observed from the

⋆E-mail: p.sanchezblazquez@uam.es

main-sequence turn-off through to the tip of the first ascent giant branch, and are not shared by the corresponding stars in the field (de Silva et al. 2009). For this reason, the primary driver responsible for these anomalous abundance patterns is thought to be 'external' and related with local environment, while 'internal' mixing mechanisms are thought to be important only in causing the variations of C and N (and possibly O) in evolved giants. Such arguments led to the postulation of the 'self-pollution' scenario (Cottrell & Da Costa 1981; Dantona, Gratton & Chieffi 1983) as being perhaps the most robust in explaining the chemical abundance anomalies in clusters (see the review of Gratton, Sneden & Carretta 2004, and references therein). According to the self-pollution scenario, a previous generation of stars polluted the atmospheres of stars observed today or provided much of the material from which those stars formed (e.g. Jehin et al. 1998; Parmentier et al. 1999; Tsujimoto, Shigeyama & Suda 2007). Several models have been proposed with intermediate-mass asymptotic giant branch (AGB) stars (e.g. Cottrell & Da Costa 1981; Denissenkov & Herwig 2003; Fenner et al. 2004; D'Antona et al. 2005; Bekki et al. 2007) and winds from massive stars (e.g. Prantzos & Charbonnel 2006; Decressin, Charbonnel & Meynet 2007a; Decressin et al. 2007b) as the most popular candidate polluters, as they provide the most simple explanation for the lack of internal spread seen in Fe and Ca in most clusters.

Hydrodynamical simulations of GC formation and evolution under the 'classical' scenario have been performed by D'Ercole et al. (2008) and Bekki (2010), although some fine-tuning to the stellar initial mass function (IMF) of the second generation – as well as the duration of the star formation – was necessary to reproduce the chemical properties and the masses of the first and second generation of stars and to prevent supernova (SN) explosions in the second generation (D'Ercole et al. 2008).

These classical scenarios still possess several problems that require solution. One of the main problems lies in understanding how a second generation can form with a current total mass comparable to the first generation, at least for the old MW GCs (see D'Ercole et al. 2008 for a discussion of the problem) without invoking an anomalous IMF (D'Antona & Caloi 2004; Decressin et al. 2007a) or extreme mass-loss from the first-generation stars during the GC evolution (by at least a factor of 10; e.g. D'Antona & Caloi 2004; Bekki & Norris 2006; Prantzos & Charbonnel 2006; D'Antona & Ventura 2007; Decressin et al. 2007a). External pollution form stars in the field (Bekki et al. 2007) have been proposed to alleviate this problem.

Other, more speculative, models have considered, for example variations in the shape of the IMF (Smith & Norris 1982; D'Antona & Caloi 2004; Prantzos & Charbonnel 2006) or significant variations to the underlying stellar structure and associated nucleosynthesis (e.g. no hot bottom burning, no third dredge up, extra mixing and/or overshooting). Such models have certainly enjoyed success in explaining certain aspects of anomalous abundance patterns in GCs (D'Antona & Ventura 2007; Bekki et al. 2007), but not in their entirety.

In summary, although the 'classical' scenario succeeds in reproducing many of the observed chemical abundance anomalies of GCs, it does still remain problematic, as does the lack of consensus concerning the dominant formation processes of GCs. As such, we considered it valuable, and indeed still do, to consider alternate, potentially viable, solutions.

In Paper I (Marcolini et al. 2009), we proposed a new, and somewhat unique, framework in which to model the chemical evolution of globular clusters. Contrary to previous 'self-pollution' models, in our framework the first stars form with 'peculiar' abundance patterns seeded by Population III pre-enrichment, while the so-called 'normal' stars form during a second phase of self-pollution from Population II Type II supernovae (SNe II). Despite being restricted to an analytical chemical evolution framework, and admittedly requiring confirmation via fully hydrodynamical simulations, we showed that our model successfully reproduced most of the well-known anti-correlations between various light elements and isotopes, while maintaining both constant iron *and* C+N+O abundances, and simultaneously recovering the empirical magnesium isotope patterns. The only major problem that the model encountered was in its underproduction of aluminium; in order to reproduce observations, a factor of 50 more Al production in intermediate-mass AGB stars was needed. We noted that such an underproduction could be accommodated within the stellar nucleosynthetic uncertainties, without compromising the predicted abundance pattern of Al in the Milky Way, via the use of Galactic chemical evolution modelling.

Our picture for globular cluster formation is predicated upon the assumption of localized pollution from a single Type Ia and $\sim$100 AGB stars. Such conditions give a qualitative explanation for the complete absence of Galactic GCs with [Fe/H] ≤ -2.4 (e.g. Harris 1996), while extremely metal-poor field stars ([Fe/H] ≤ -3.0) exist in copious numbers (e.g. Frebel et al. 2007 and references therein).

In Paper I, emphasis was placed on the evolution of the light elements within several intermediate-metallicity ([Fe/H] ~ -1.4) GCs (NGC 6752, M13 and NGC 2808). In Paper II, we now extend the application of the model to both the more metal-poor (M15 and NGC 6397, with [Fe/H] $= -2.26$ and -1.95, respectively; Harris 1996) and metal-rich (47 Tuc, with [Fe/H] $= -0.76$) regimes. In light of the availability of recent observational work, we also explore the behaviour of fluorine in M4, and the iron-peak elements (and isotopes) for NGC 6752 and 47 Tuc. In Section 2, we discuss our adopted stellar yields, while in Section 3 the framework is summarized. Our results, both globally and on a cluster-by-cluster basis, are presented in Sections 4–7.

2 STELLAR YIELDS

As discussed in Paper I, we employ an IMF-weighted yield distribution for our chemical evolution predictions, based upon four sets of SNe II models, spanning the mass range 10–60 $M_{\odot}$ (Woosley & Weaver 1995; Chieffi & Limongi 2004; Kobayashi et al. 2006), as summarized in Table 1. Therein, we only show the new elements analysed in this paper; we refer the reader to tables 1 and 2 of Paper I for the elements discussed in our earlier work. While in a global sense, the various yields are in reasonable agreement (particularly for the α-elements), there are obviously those for which factors of $\sim$3 variations exist (e.g. several of the iron-peak elements, for which the sensitivity to the mass cut is most extreme). As in Paper I, an average yield is derived by averaging between the compilations when agreement exists to within a factor of 2; otherwise an admittedly arbitrary decision was made to adopt the compilation that best reproduces the abundances of low-metallicity ($-2.0 \leq$ [Fe/H] ≤ -1.0) halo stars (e.g. Gratton et al. 2000). The element with the largest variation is that of fluorine; this is due to the inclusion of the neutrino process by Woosley & Weaver (1995) that increases by more than an order of magnitude the production of light elements (including ^{7}Li and ^{19}F) (see Timmes, Woosley & Weaver 1995 for further discussions). In this case, we use the yields of Woosley & Weaver (1995). Unless stated differently, in

Table 1. Mean SNe II stellar yields averaged over the progenitor mass range 10–60 $M_\odot$ for a Salpeter (1955) IMF for several compilations: W&W = Woosley & Weaver (1995); C&L = Chieffi & Limongi (2004); KOB = Kobayashi et al. (2006). The yields of Fe are given in solar masses while for different elements we show the $[X_i/Fe]$ ratio.

SNe type	Fe	[F/Fe]	[Si/Fe]	[Ca/Fe]	[Ti/Fe]	[V/Fe]	[Co/Fe]	[Ni/Fe]	[Cu/Fe]
W&W ($Z = 0.0002$)	6.1e–2[a]	−0.29	+0.45	+0.31	−0.06	−0.29	−0.01	+0.26	−0.55
W&W ($Z = 0.002$)	6.9e–2[a]	+0.11	+0.42	+0.28	−0.13	−0.21	+0.12	+0.30	−0.37
C&L ($Z = 0.0001$)	1.0e–1	−2.69	+0.62	+0.54	−0.22	−0.31	−0.39	+0.34	−0.55
C&L ($Z = 0.0001$)	1.0e–1	−1.57	+0.60	+0.51	−0.15	−0.47	−0.26	+0.23	−0.68
KOB ($Z = 0.001$)	7.5e–2	−1.08	+0.60	+0.35	+0.03	−0.31	−0.35	−0.35	−0.39
KOB ($Z = 0.001$+HN)	1.1e–1	−1.20	+0.57	+0.28	−0.13	−0.25	−0.17	−0.21	−0.41
Model (SNe II)	9.0e–2	+0.00	+0.40	+0.30	−0.05	−0.30	+0.00	+0.00	−0.55

Table 2. Mean SNe II, SNe Ia and intermediate-mass AGB yields in solar masses. The SNe II entry corresponds to the adopted 'average' Model is listed at the end of Table 1. The SNe Ia yields correspond to the models described by Iwamoto et al. (1999). The mean AGB yields (from Karakas & Lattanzio 2007) are averaged over the progenitor mass range 4–7 $M_\odot$ assuming a Salpeter (1955) IMF.

SNe type	Fe	F	Si	Ca	Ti	V	Co	Ni	Cu
SNe II (Model)	9.00e–2	3.00e–5	1.28e–1	9.40e–3	2.23e–4	1.33e–5	2.45e–4	5.33e–3	1.33e–5
SN Ia (W7)	7.49e–1	5.67e–10	1.56e–1	1.19e–2	3.43e–4	7.49e–5	1.04e–3	1.26e–1	3.00e–6
SN Ia (WDD1)	6.72e–1	1.70e–9	2.74e–1	3.10e–2	1.13e–3	1.33e–4	3.95e–4	3.40e–2	6.92e–6
SN Ia (CDD1)	6.48e–1	5.83e–10	2.79e–1	3.18e–2	8.18e–4	1.11e–4	2.91e–4	3.50e–2	7.28e–7
AGB (model)	2.27e–5	4.98e–9	4.87e–5	0.0	0.0	0.0	7.93e–8	3.07e–6	0.0

the following we refer to the yields given in Table 1 as the 'model' yields.

In Table 2, we summarize the mean yields for intermediate-mass AGB stars (see complementary table 3 of Paper I for the elements studied in our earlier work) calculated by averaging over a Salpeter (1955) IMF, in the mass range 4–7 $M_\odot$, the Karakas & Lattanzio (2007) yields with $Z = 0.0001$ (we refer to this model as the 'reference model'). There are several Fe-peak elements which were not considered by these authors (i.e. Ca, Ti, V and Cu) and, for this work, we have therefore assumed that these elements are not synthesized in significant quantities in intermediate-mass AGB stars.[1]

For SNe Ia we use the yields of Iwamoto et al. (1999) and explore the impact of various stellar physics treatments, including slow deflagration (W7) and delayed detonation models (WDD1 and CDD1). While SNe Ia produce small amounts of light elements (relative to SNe II), they can produce significant amounts of heavier α-elements (e.g. Si, Ca and Ti) and Fe-peak elements. The specific yield of the latter amount depends upon the deflagration speed and ignition densities, with the different models producing yields that span a factor of 4 (see Table 2 and, more importantly, the original paper of Iwamoto et al. 1999 for details).

3 MODEL

The details of the models are described in Paper I; here, we briefly review the main characteristics. The model has two phases: first, the localized effect of intermediate-mass AGB field stars and a single SN Ia explosion produce an inhomogeneous pollution that is added to an interstellar medium (ISM) that was previously enriched by very low metallicity SNe II. Since the peak of the SN Ia rate has a time-scale (∼70–80 Myr; e.g. Matteucci & Recchi 2001; Mannucci, Della Valle & Panagia 2006) comparable with the lifetime of a 5-$M_\odot$ star (Schaller et al. 1992; Karakas & Lattanzio 2007), such pre-enrichment is not a priori unreasonable (Paper I provides a detailed discussion of the initial conditions). The formation of a proto-GC takes place inside this chemically peculiar region; the stars formed during this phase will have 'peculiar' chemical properties compared with 'normal' field stars of the same metallicity.

As star formation proceeds, new SNe II explode, polluting the gas with the product of their nucleosynthesis. This represents the second phase of the model. The stars formed in this phase will have chemical properties that are more similar to the field stars of the same metallicity (henceforth referred to as 'normal'). Eventually, the occurrence of SNe II explosions quenches further star formation and the GC evolves passively. A schematic of the model is shown in Fig. 1.

During the evolution there are two mechanisms that govern the chemical properties of the forming stars. We showed in Paper 1 that the two mechanisms act together to regulate the [Fe/H] abundance, which is kept essentially constant throughout a cluster's evolution. Furthermore, the general chemical properties of the stars forming in this region evolve from 'peculiar' to that more typical of essentially 'pure' SNe II enrichment, which is the opposite to what is normally assumed in self-enrichment models.

The final chemical properties of the GC are controlled by three parameters: the size of the inner region where the SN Ia is confined (R_{in}), the initial number of AGB stars (N_{AGB}) and the abundance of the ISM of the halo ($[Fe/H]_{ISM}$). Table 3 lists these parameters for the globular clusters examined in this paper. We can see that

[1] We note here in passing that our preliminary work now suggests that low-metallicity, massive AGB stars can produce a substantial amount of copper, i.e. one 5 $M_\odot$, $Z = 0.004$ model we have generated produced [Cu/Fe] ∼ +0.8. A larger grid of models will be required before we can assess its global importance within the context of our GC modelling efforts.

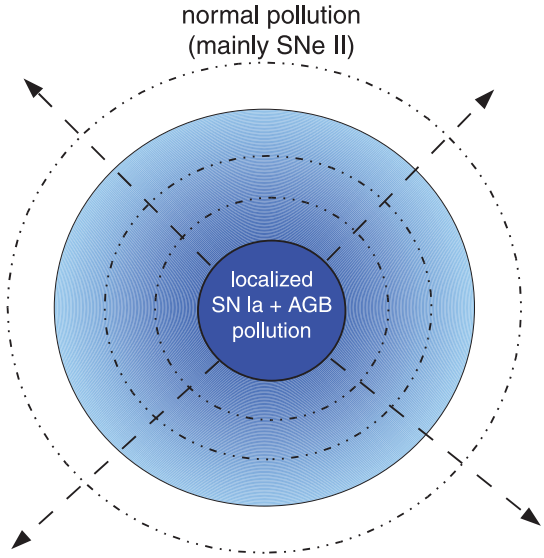

Figure 1. Schematic of the model outlined in Paper I. Initially, a localized volume (inner blue region; solid line) pre-enriched with Population III ejecta is polluted by a single SN Ia and ∼100 intermediate-mass AGB stars. After a new generation of stars is born, associated SNe II begin to pollute and expand the inner volume, while mixing concurrently with the surrounding lower-[Fe/H] ISM.

Table 3. Initial conditions of the models for the different globular clusters.

	$[Fe/H]_{ISM}$	$[Fe/H]_{in}$	R_{in} (pc)	N_{AGB}
M15	−3.30	−2.35	65	150
NGC 6397	−3.20	−2.05	49	150
NGC 6752	−2.55	−1.60	36	250
M4	−1.65	−1.15	29	130
47 Tuc	−1.40	−0.75	20	140
M13	−3.50	−1.50	31	170
NGC 2808	−2.85	−1.10	24	180

for these models, there is an inverse correlation between the value of the surrounding $[Fe/H]_{ISM}$ and the confinement radius of the SN Ia, R_{in}.[2] Such an inverse correlation is consistent physically with the expected inverse correlation between metallicity and cooling efficiency. The higher the metallicity of the confining ISM, the more efficient the cooling and energy dissipation, and the more confined the SN remnant's expansion will be. A factor of 100 increase in metallicity would make the radius at which the remnant merges with the ISM a factor of 3 smaller and, therefore, the enrichment will be spread over a smaller volume (Gibson 1994).

To illustrate the effect of the model-free parameters on the observed O–Na anti-correlation, we show in Fig. 2 models changing the number of AGB polluters, the initial radius (R_{in} and the initial iron content of the ISM $[Fe/H]_{ISM}$, together with a collection of observational data for different GCs (Kraft et al. 1993; Sneden et al. 1997; Ivans et al. 2001; Ramírez & Cohen 2003; Sneden et al. 2004; Cohen & Meléndez 2005; Yong et al. 2005; Carretta et al. 2006; Koch & McWilliam 2008). We also show three different models with $N_{AGB} = 100$, 160 and 250 and $R_{in} = 40$, 30 and 20 pc. It can be seen that appropriate choices for the initial conditions are able to reproduce both the trend and the associated 'scatter' in the observed O–Na anti-correlation.

[2] Admittedly, the correlation is not a particularly strong one, particularly when the two models from Paper I (bottom two entries of Table 3) are included.

4 VERY METAL-POOR AND METAL-RICH GCs

4.1 The case of very-metal-poor GCs: M15 and NGC 6397

In Fig. 3 we show the [Na/Fe]–[O/Fe] and the [N/Fe]–[C/Fe] evolution predicted by our models for M15 and NGC 6397 together with the corresponding observational data sets of Sneden et al. (1997), Cohen & Meléndez (2005) and Carretta et al. (2005). Table 3 lists the model parameters inferred which best fit the overall [Fe/H] content of NGC 6397 and M15. To fit the abundances for these clusters, a larger value of R_{in} and a lower value of $[Fe/H]_{ISM}$ were needed, relative to those employed for the more metal-rich GCs. The models recover the O–Na anti-correlation for both clusters, but are less successful in doing the same for the C–N anti-correlation. This was discussed in Paper I, where we showed that while the main contribution to the production of carbon and nitrogen comes from intermediate-mass AGB stars, the amount of nitrogen produced by these stars is much larger than that of carbon. The result is that while the initial AGB production of carbon is offset by the Fe deposited by the SN Ia, the [N/Fe] ratio can reach values as high as 1.5 dex. For this reason, while the carbon content remains practically constant during the evolution (solid lines), the nitrogen content varies by more than an order of magnitude (see right-hand panels of Fig. 3). As a consequence, our reference models (solid lines) are able to reproduce the observed spread in N while keeping C constant. However, in order to obtain an anti-correlation between the relative abundance of these elements, the production of C by AGB stars needs to be reduced by a factor of 4 (dashed lines in Fig. 3).

It can also be seen that the absolute values of [C/Fe] for NGC 6397 are somewhat difficult to reproduce in our model, particularly at low [N/Fe] values. However, the comparison with carbon and nitrogen measurements needs to be done with caution. The abundances in NGC 6397 have been derived from spectra of slightly evolved stars (subgiants). The surface abundances of these elements are affected by internal mixing and may not reflect the composition of the ISM when those stars formed (see Smith & Tout 1992; Charbonnel 1994, 1995; Denissenkov & Tout 2000; Weiss, Denissenkov & Charbonnel 2000; Gratton, Sneden & Carretta 2004, and reference therein). The carbon abundance measurements of M15 and NGC 6397 differ by ∼0.3 dex (see right-hand panel of Fig. 3). This is very difficult to understand given the similarities in their overall metallicity and nitrogen content. We have assumed here that this offset is artificial and perhaps reflects a systematic error in the carbon measurements of NGC 6397, but admit that this remains, for now, just an assumed interpretation. If we apply an offset to the carbon abundances of the NGC 6397 stars to match the abundances of M15 stars, our model agrees better with the observations (Fig. 3).

4.2 The case of metal-rich GCs: 47 Tuc

As a final test for the evolution of the abundances of light elements, we consider the case of the metal-rich globular cluster 47 Tuc ([Fe/H] = −0.67) (e.g. Carretta et al. 2004). In order to match its chemical properties we assume that the initial SN Ia was quite localized ($R_{in} = 20$ pc) and that the Fe content of the ISM of the halo

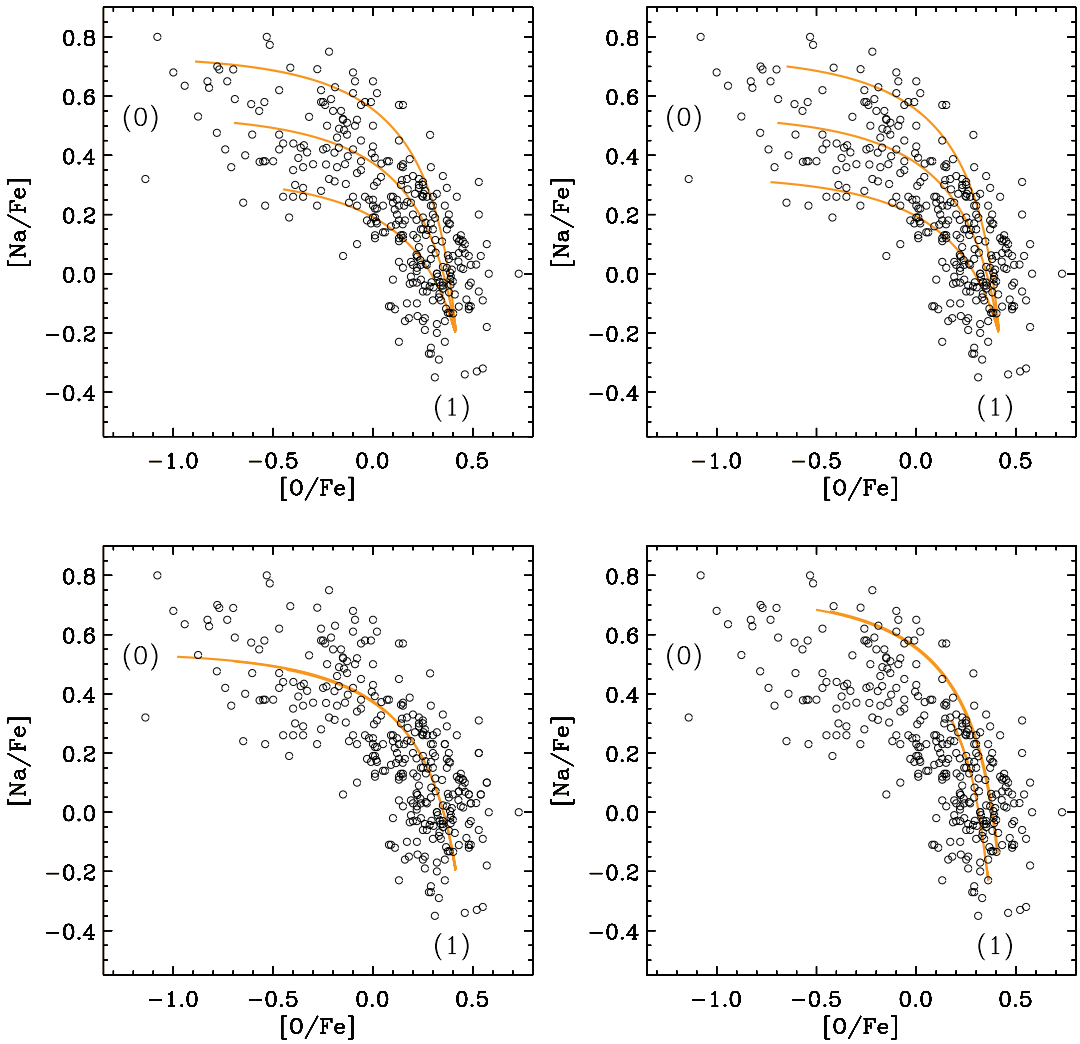

Figure 2. Representative model predictions for the O–Na anti-correlation. The first generation of stars is born with peculiar chemical properties (i.e. low [O/Fe] and high [Na/Fe]). Once the first SNe II start to explode, polluting and expanding the inner region, the chemical properties of the forming stars evolve towards 'normal' values typical of pure SNe II pollution (i.e. high [O/Fe] and low [Na/Fe]). Upper left-hand panel: the three lines represent models with different initial conditions – i.e. models in which the number of intermediate-mass AGB stars and the initial radius of the inner pre-polluted region have been changed to match the observational scatter observed in different GCs (small circles; see text for more details about the data sets). The solid lines represent models with the combinations of values of $N_{\rm AGB} = 100$, 160 and 250 and $R_{\rm in} = 40$, 30 and 20 pc with the former (latter) values representing the lower (upper) line. Upper right-hand panel: the three lines correspond to the models with the same inner radius ($R_{\rm in} = 30$ pc), but with different number of AGB stars: $N_{\rm AGB} = 100$, 160 and 250, from lower to upper line, respectively. Bottom left-hand panel: the three lines reflect the effect of changing the inner radius, keeping the number of AGB stars fixed to $N_{\rm AGB} = 160$. Bottom right-hand panel: effect of changing the $[{\rm Fe/H}]_{\rm ISM}$ keeping the rest of the parameters fixed. From top to bottom $[{\rm Fe/H}]_{\rm ISM} = -3.30$, -2.55 and -1.40.

at the epoch of formation was higher than that for the metal-poor GC ($[{\rm Fe/H}]_{\rm ISM} = -1.40$). This value is in the range of iron metallicities encountered in the Galactic halo ($-4.0 \geq [{\rm Fe/H}] \geq +0.0$ peaking near $[{\rm Fe/H}] \simeq -1.7$; e.g. Ryan & Norris 1991). For the specific case of 47 Tuc we have used the $Z = 0.004$ yields, consistent with its higher initial metal content.

The evolution of the O–Na and C–N anti-correlations is plotted in Fig. 4 together with the observational data of Carretta et al. (2005), Alves-Brito et al. (2005) and Briley et al. (2004). Again, the anti-correlations are better reproduced once we assume that the carbon production in AGB stars is reduced by a factor of 4 compared with the theoretical values of Karakas & Lattanzio (2007). There is also an evident offset of 0.15 and 0.4 dex between the measurements of carbon and nitrogen derived by Carretta et al. (2005) and Briley et al. (2004). While it is beyond the scope of this paper to understand the origin of these offsets, our assumed yields are in agreement with the values obtained by Carretta et al. (2005) but, again, the model has no problem in being able to reproduce the trend from Briley et al. (2004, dotted line).

4.3 [Fe/H] evolution

Fig. 5 shows that in agreement with the results of Paper I for intermediate-metallicity GCs, [Fe/H] remains constant during the evolution of metal-poor *and* metal-rich globular clusters. (Note that we choose to plot [Na/Fe] instead of the usual [O/Fe] because most of the oxygen values for this cluster are upper limits.)

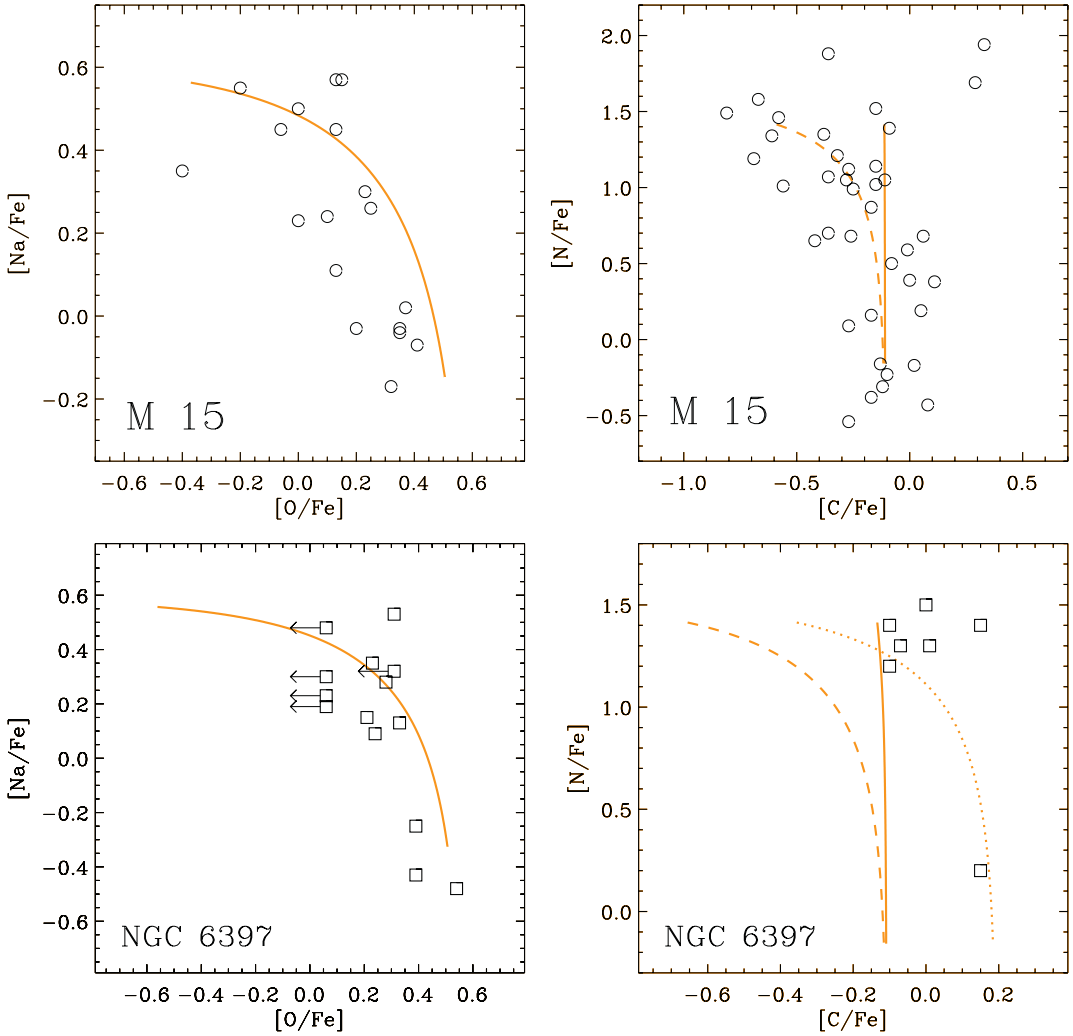

Figure 3. Upper left-hand panel: evolution of [Na/Fe] versus [O/Fe] for the model of M15 (solid line) plotted against the data by Sneden et al. (1997). Upper right-hand panel: evolution of [N/Fe] versus [C/Fe] for the same model (reference model, solid line) plotted against the data by Cohen & Meléndez (2005). Dashed line indicates the effect of reducing the production of C by AGB stars by a factor of 4. Lower panel: same but showing the evolution of the NGC 6397 model, plotted together with the observational data by Carretta et al. (2005). Note that in this case most of the lowest [O/Fe] abundances are upper limits. The dotted line in the lower right-hand panel corresponds to the same evolution of the dashed line (reference model with a reduced production of C by AGB stars) but offset by 0.3 dex (see text for details).

5 M4 AND ITS FLUORINE CONTENT

Fluorine abundances have been derived for the stars of M4 by Smith et al. (2005), finding they vary by a factor of 6, correlate with oxygen and anti-correlate with sodium and aluminium. Fluorine yields are a strong function of stellar mass and, therefore, can be used to constrain the nature of the polluters in globular clusters. Fluorine, like oxygen, is scarcely produced in intermediate-mass AGB stars (F is destroyed in 5–6 $M_{\odot}$ and produced in the 4 $M_{\odot}$ models of Karakas & Lattanzio 2007) and here is mainly synthesized by the SNe II models.

As is evident in the lower panels of Fig. 6, where we plot the observational data alongside the predicted evolution of our model, fluorine correlates with oxygen and is anti-correlated with sodium. In our model, [F/Fe] evolves from an initially subsolar value to a slightly supersolar value, typical of SNe II pollution, and in agreement with the observational constraints. Smith et al. (2005) argue that the correlations can be explained within a self-polluting scenario in which AGB stars act as the main polluters. However, the destruction of fluorine by intermediate-mass AGB stars does not appear sufficient to explain the 'final' extreme low values of the [F/Fe] ratio. In our model, these values are expected in the *first* stars formed, due to the inhomogeneous SN Ia effect.

6 OTHER ELEMENTS

6.1 Heavy α-elements

While there are multiple observations of light-element abundances in GCs, only recently have heavier elements become accessible for statistically significant samples of stars. Yong et al. (2005) measured 20 elements in 38 bright giants of NGC 6752, while Carretta et al. (2004) reported the abundances of nine subgiants and three dwarfs of 47 Tuc, both for α-elements and Fe-group elements. While light elements show the already discussed variations spanning in some cases more than an order of magnitude, silicon and heavier elements ($X_{\rm heavy}$) show much smaller star-to-star scatter in their [$X_{\rm heavy}$/Fe]

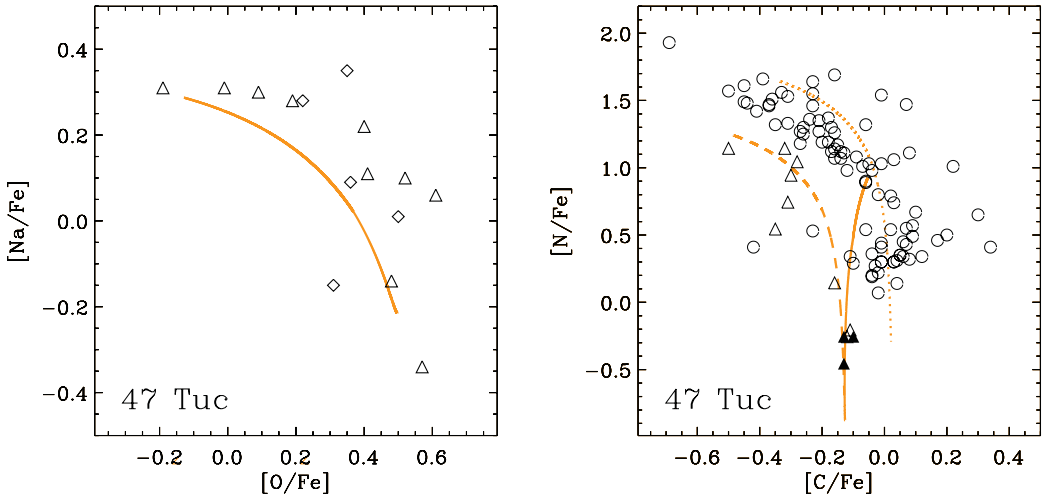

Figure 4. Left-hand panel: evolution of [Na/Fe] versus [O/Fe] for the reference model for 47 Tuc plotted against the observational data collected by Carretta et al. (2005, triangles) and Alves-Brito et al. (2005, diamonds). Right-hand panel: evolution of [N/Fe] versus [C/Fe] for the same model plotted against the values presented in Carretta et al. (2005, triangles) and Briley et al. (2004, circles). Dashed line indicates a model where the production of C by AGB stars has been reduced by a factor of 4 with respect to the reference model. In the case of Carretta et al. (2005), open triangles refer to subgiant stars while filled triangles refer to dwarf stars. The dotted line in the right-hand panel corresponds to the dashed-line model offset by 0.15 dex in carbon and 0.40 dex in nitrogen.

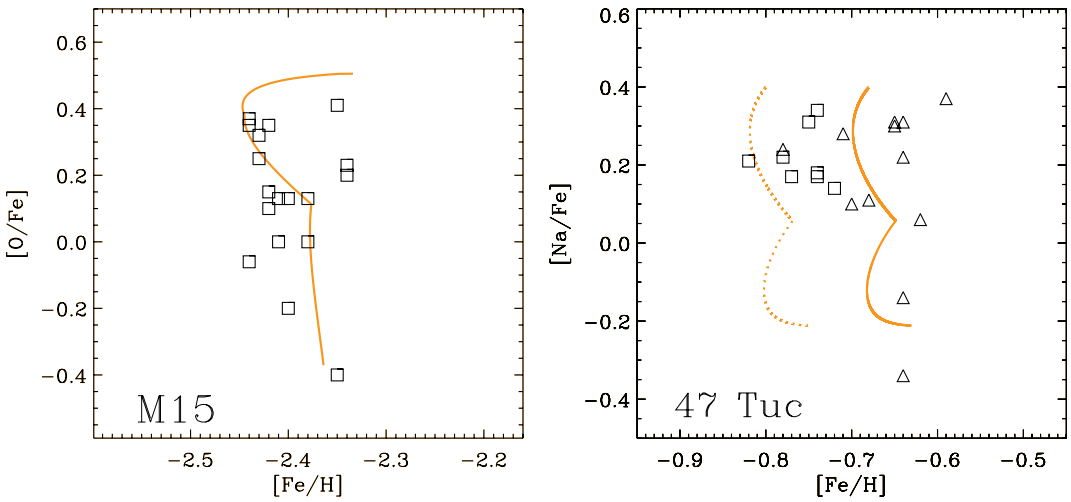

Figure 5. Left-hand panel: evolution of [O/Fe] versus [Fe/H] for the model of globular cluster M15 compared with the observational data set from Sneden et al. (1997). Right-hand panel: evolution of [Na/Fe] versus [Fe/H] for the model of globular cluster 47 Tuc compared with the observational data sets of Carretta et al. (2004, triangles) and Koch & McWilliam (2008, squares). For these very metal-poor and metal-rich GCs, [Fe/H] remains roughly constant throughout their respective evolution.

ratio. This smaller scatter is consistent, in most cases, with measurement uncertainties. Furthermore, the mean [$X_{\rm heavy}$/Fe] ratios are consistent with field stars of the same metallicity. There is some evidence for heavy α-elements correlating with lighter elements; Yong et al. (2008) found a statistically significant, although loose, correlation between silicon and aluminium in NGC 6752, noting that the Si abundances are roughly constant from star to star.

In Fig. 7 we plot the evolution of the [X_i] ratio of different α-elements versus the [O/Fe] for the model of NGC 6752, together with the observational values obtained by Yong et al. (2005). As can be seen, our model is able to reproduce reasonably well the spread in the O–Mg correlation. The different lines in Fig. 7 represent models with different prescriptions for the SN Ia yields of Iwamoto et al. (1999): W7 (model with slow central deflagration), WDD1 (model with fast deflagration), and CDD1 (model delayed detonation in the outer layer). As can be seen, the abundance of the Fe-group elements (in particular, the neutron-rich species such as ^{50}Ti, ^{58}Fe and ^{58}Ni) depends considerably upon the chosen physics of the model. From Table 2, it is evident that variations in the SNe Ia yields by up to a factor of 4 are possible for these elements.

Intermediate-mass AGB stars produce some Mg – mostly in the form of the neutron-rich isotopes (Fenner et al. 2003) – and thus even if a variation of $\sim$1 dex is achieved in [O/Fe], only a mild depletion of 0.3 dex in [Mg/Fe] is present due to the AGB contribution. The Mg production in different SN Ia models is roughly the same, although it is small compared to the production of Mg in SNe II and AGB stars.

An apparent failure of our model is that the 'shape' of the O–Mg correlation is 'concave', while it looks to be more 'convex' in the

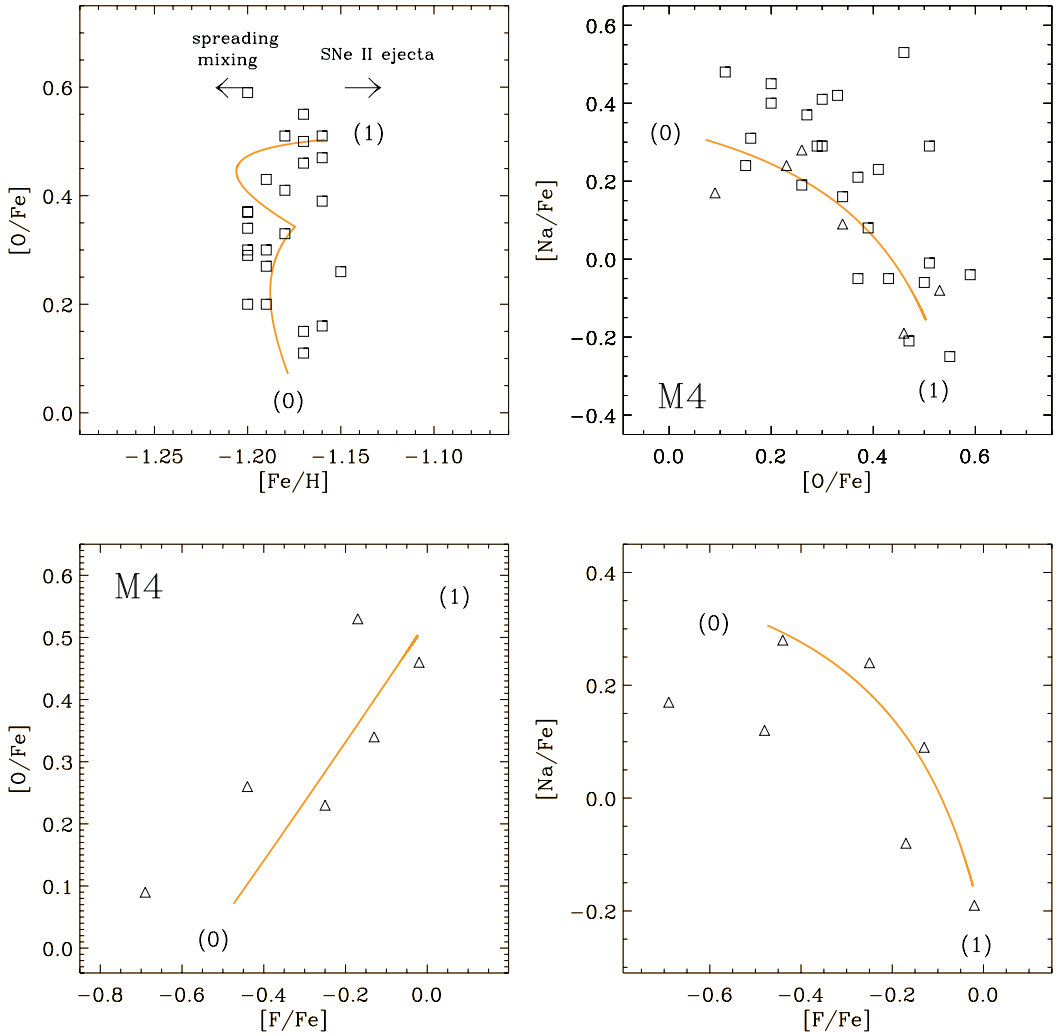

Figure 6. Evolution of various element ratios for the model for globular cluster M4; comparison observational data from Ivans et al. (1999, squares) and Smith et al. (2005, triangles). Upper left-hand panel: evolution of [O/Fe] versus [Fe/H]. Upper right-hand panel: evolution of [Na/Fe] versus [O/Fe]. Lower left-hand panel: evolution of [O/Fe] versus [F/Fe]. Lower right-hand panel: evolution of [Na/Fe] versus [F/Fe].

observational data (upper left-hand panel in Fig. 7). This may be due to the fact that we are using averaged yields for SNe II. Indeed more massive SNe II progenitors produce much larger amount of Mg and explode earlier, explaining why the empirical [Mg/Fe] increases quite quickly, at apparent odds with our model.

While the contribution from the SN Ia is not relevant for Mg, this is not the case for the other heavier α-elements. Indeed, Table 2 shows that an SN Ia produces more Si, Ca and Ti than a single SN II (note however that their production ratio against iron, [X_i/Fe], is lower than that for the case of SNe II and is usually subsolar). Moreover, variations in the initial value of the ratio [X_i/Fe] (up to 0.2 dex for Si and 0.4 dex for Ca and Ti) are possible when testing different SNe Ia models, even if all these values remain, more or less, subsolar (see Fig. 7). In addition, our models predict a correlation between Si–O and Ca–O, with variations of up to ∼0.5 dex in the [Si/Fe] abundance and ∼0.3 dex for [Ca/Fe] (for models CDD1 and WDD1). These predicted correlations are not in agreement with the observational constraints. Adopting the W7 model increases the scatter, only making the situation worse.

For Ti, the models CDD1 and WDD1 maintain the [Ti/Fe] abundance at a roughly constant value, consistent with the observations (even if there is an intrinsic offset of ∼0.2 dex; dashed line in the bottom right-hand panel of Fig. 7). In contrast, model W7 produces [Ti/Fe] abundances that do not agree with the observations. Since Ca is not synthesized in intermediate-mass AGB stars, we investigate how much Ca production we would require in (very) metal-poor SNe Ia to fit the observational constraints. Indeed, a factor of 2 more Ca production in (very) low metallicity SN Ia[3] compared with the WDD1 model (green line in Fig. 7) is able to reconcile our model with observations. Note that the fact the [Ca/Fe] ratio in halo field stars is observed to decline with [Fe/H] implies that the Ca yields of Iwamoto et al. (1999) are consistent with SN Ia at larger metallicity.

The same experiment can be made for Si, but in this case we should also try to take into account a possible higher AGB contribution. As already discussed, Yong et al. (2005) found a statistically significant correlation (at odds with our model) between [Si/Fe] and [Al/Fe] which, in their interpretation, can be explained if the reaction ^{27}Al(p,γ)^{28}Si is favoured over ^{27}Al(p,α)^{24}Mg. Hot-bottom burning

[3] Or just the prompt SNe Ia which explode on time-scales shorter than ∼100 Myr.

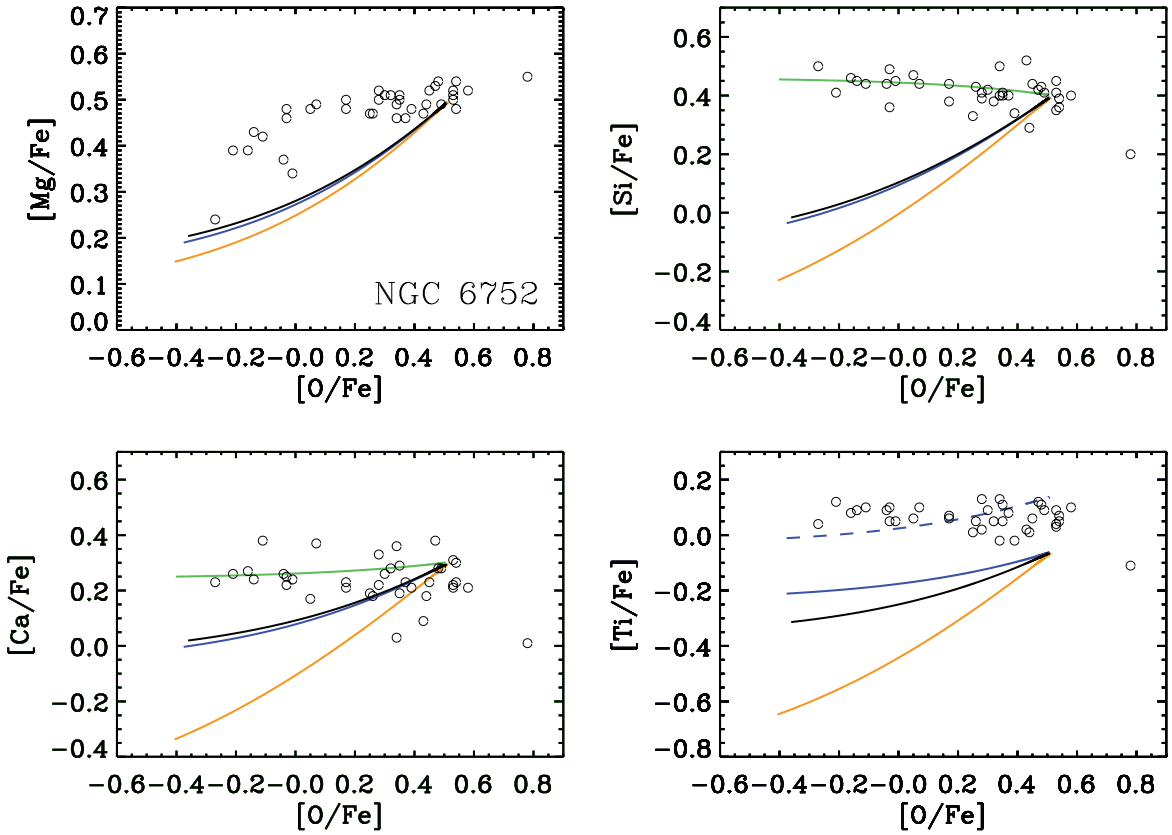

Figure 7. Evolution of different α-elements ([Mg/Fe], [Si/Fe], [Ca/Fe] and [Ti/Fe]) versus [O/Fe] for the case of NGC 6752. Open circles correspond to the observational data set from Yong et al. (2005). The colour-coded lines correspond to models with different SNe Ia yields. Orange lines: W7; blue lines: WDD1; black lines: CDD1. The green lines represent a model in which the Si and Ca yields have been increased of a factor of three and two, respectively, compared with the yields of model WDD1. The dashed blue line in the lower right-hand panel is the corresponding blue solid line, offset by 0.2 dex.

(HBB) in intermediate-mass AGB stars is expected to produce small amounts of ^{28}Si from proton capture on ^{27}Al, though the Si yields are expected to be small (Karakas & Lattanzio 2003, 2007). The Si production depends on the temperature of the HBB region and also on the assumed reaction rates. Again, similar to Ca, the problem of Si can be solved with a higher production of Si in (very) low metallicity SN Ia[4] and/or a higher Si production in AGB stars [a mean value of $3.5 \times 10^{-3}\,M_{\odot}$ (compared to $4.8 \times 10^{-5}\,M_{\odot}$ predicted by Karakas et al. 2008)]. Note that this is *exactly* the value of Al we needed in Paper I to reproduce the Al–Mg anti-correlation in this GC. *If* our framework is correct, it means that current intermediate-mass AGB models are underestimating the yields of Al and Si by 1–2 orders of magnitude.

From Fig. 8, we see that are no serious issues in reproducing the same α-elements for the more metal-rich cluster 47 Tuc.[5] In this case, the collection of subgiants and dwarfs from Carretta et al. (2004) is consistent with our model. We should note that due to the higher SNe II pre-enrichment ($[Fe/H]_{ISM}$), this model does not reach the low values of [O/Fe] seen in the NGC 6752 model. In this case, the Iwamoto et al. (1999) yields have no problem in fitting the observational data set. In our framework, 47 Tuc should form later than NGC 6752 (i.e. from a more metal-rich ISM) and the suggestion that very low metallicity SN Ia (or AGB) may have slightly different (up to a factor of 4) Si and Ca yields is plausible. In this case, the temporal evolution goes from high values of [Na/Fe] to low values.

6.2 Fe-peak elements

SNe Ia and SNe II synthesize a significant fraction of the Fe-group elements, while intermediate-mass AGB stars contribute very little to the same. The analysis of $[X_i/Fe]$, where X_i represents an Fe-peak element, can prove extremely useful in understanding the relative contributions of the two types of supernovae. The ratio of iron produced in SNe Ia-to-SNe II is $Fe_{SNe\,Ia}/Fe_{SNe\,II} \simeq 7$–8 (depending on the adopted yields); *if* $[X_i(SN\,Ia)/X_i(SN\,II)] < 7$–8, then $[X_i/Fe]$ will increase during the GC evolution and vice versa.

Fig. 9 compares the results of our models for Fe-group elements (specifically V, Co, Ni and Cu) with the corresponding observational data of Yong et al. (2005), for the case of the globular cluster NGC 6752. [V/Fe] and [Ni/Fe] remain roughly constant, in good agreement with observations, when using the WDD1 and CDD1 models. Using the W7 model for SN Ia, though, produces less V and more Ni than needed to keep [Ni/Fe] and [V/Fe] constant, leading to variations of 0.2 and 0.4 dex for [V/Fe] and [Ni/Fe], respectively (see Table 2). The trend in the evolution of Co is well reproduced (apart from a small ∼0.1 dex offset) by using SNe Ia model W7,

[4] Or, again, prompt SN Ia; as before, the value of [Si/Fe] $\sim +0.0$ in field stars at solar metallicity implies that at higher metallicity, the Iwamoto et al. (1999) yields are correct (but note that these yields are calculated for solar metallicity).

[5] In Fig. 8, we have shown the [α/Fe] trends against [Na/Fe], rather than [O/Fe], as the majority of the stars in the Carretta et al. (2005) sample either have non-detections or only upper limits to their oxygen abundances.

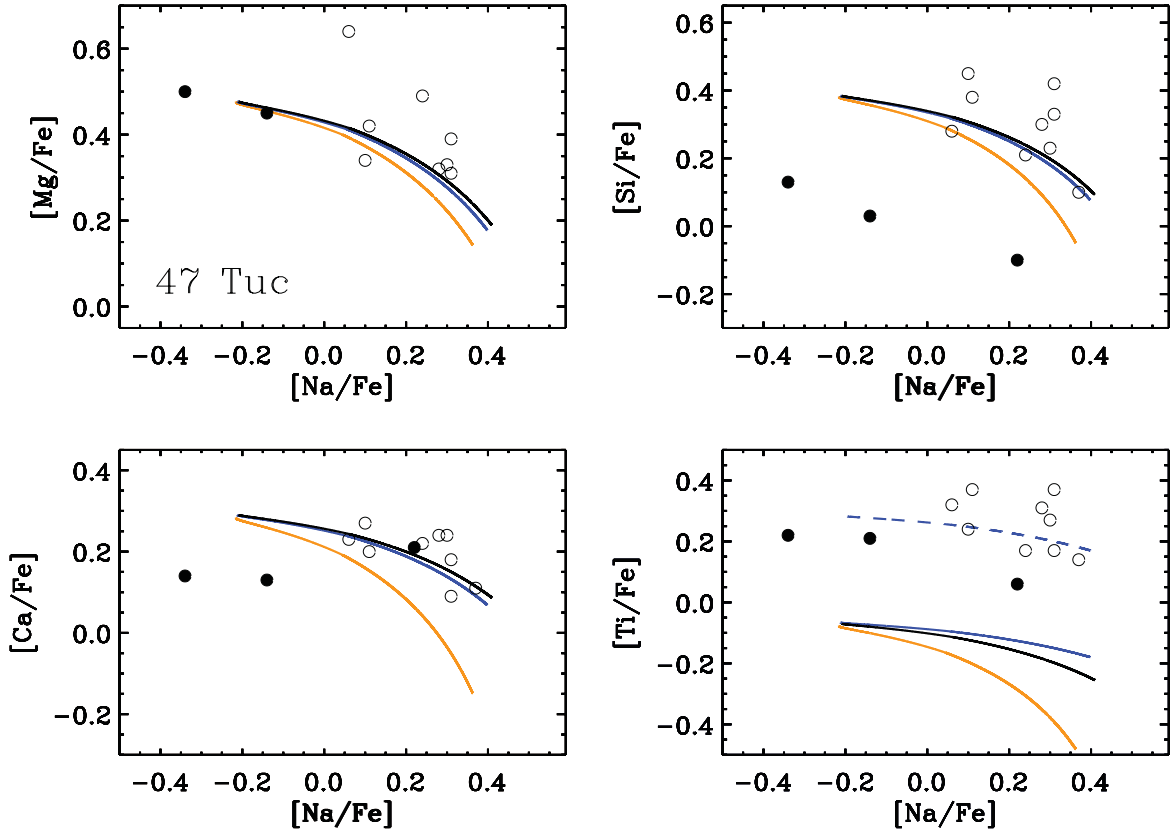

Figure 8. Evolution of different α-elements ([Mg/Fe], [Si/Fe], [Ca/Fe] and [Ti/Fe]) versus [Na/Fe] for the case of 47 Tuc. Open circles correspond to the observational data set from Carretta et al. (2005); the filled symbols are the three dwarfs, while the open symbols are the nine subgiants. The colour-coded lines correspond to models with different SNe Ia yields. Orange lines: W7; blue lines: WDD1; black lines: CDD1. The dashed line in the bottom right-hand panel corresponds to the [Ti/Fe] prediction using the WDD1 SNe Ia model, but offset by ∼0.3 dex (see text for details).

while the others underestimate its production by roughly a factor of 2.

In the lower two panels of Fig. 9, we compare the [V/Fe] and [Ni/Fe] evolution of our model for the metal-rich GC 47 Tuc, with the data presented in Carretta et al. (2005). The models underproduce vanadium by a factor of 2 and overproduce nickel by ∼0.2 dex. We note in passing that observationally the two clusters themselves differ in their mean [V/Fe] by ∼0.3 dex. The origin of this difference remains unclear and in the lower left-hand panel of Fig. 9, we show our model predictions for the 47 Tuc [V/Fe]–[Na/Fe] evolutionary trend. We show the same curves offset by ∼0.3 dex, to coincide with the data. We cautiously suggest that our model can (roughly) match the evolution of most of the Fe-group elements analysed, within the theoretical uncertainties of SNe yields, and those associated with the observational data.

Having just made that conclusion though, one notable exception exists in the form of copper. Indeed, while the observed Cu content for NGC 6752 seems to be roughly constant, our model predicts a very strong correlation with oxygen, independent of the chosen SNe Ia model. From the middle right-hand panel of Fig. 9, we see that the initial [Cu/Fe] ratio is greatly underestimated in our models, for any choice of the SNe Ia yields: all the SNe Ia models analysed here produce very little copper (see Table 2). The origin of the copper observed in field halo stars remains a matter of debate and, at this stage, the magnitude of this apparent failure of the model needs to be confirmed/refuted with additional empirical data. *Assuming* a value for SNe Ia copper production of $1.2 \times 10^{-4}\,M_{\odot}$ would bring the models in agreement with the extant data. It is very interesting to note that such a suggestion is not entirely without precedent; indeed, this value is very similar to the one ($0.5–2.0 \times 10^{-4}\,M_{\odot}$) proposed by Matteucci et al. (1993) to reproduce the [Cu/Fe] versus [Fe/H] trend for MW stars (but see also Romano & Matteucci 2007). In addition, Mishenina et al. (2002), analysing the copper abundance trend in 90 metal-poor stars in the metallicity range $-3.0 \geq$ [Fe/H] ≥ -0.5, found evidence that SNe Ia must play a significant role (>65 per cent) in producing copper.

Yong et al. (2008) pointed out that even if the abundance of Fe-peak elements shows a small scatter in NGC 6752, their values statistically correlate with nitrogen. This is exactly what we expect in our model, even if the exact slope and scatter of this correlation depends upon the interplay between an SN Ia origin and an SN II elemental origin.

7 ISOTOPE RATIOS AS AN OBSERVATIONAL TEST TO VALIDATE THE FRAMEWORK

In Paper I, we tested our model predictions for the behaviour of Mg isotopes in GCs against measured isotope abundances in NGC 6752 and M13. Our framework succeeded in reproducing their observed trends, but we require a better test to verify the SN Ia framework of our model (recall that Mg is not a strong constraint for the SN Ia framework, as its origin is linked to SNe II and AGB stars). The purpose of this section is to make predictions regarding isotope ratio of heavy elements where the imprint of an SN Ia should be more important; this can constitute a definitive test for the model.

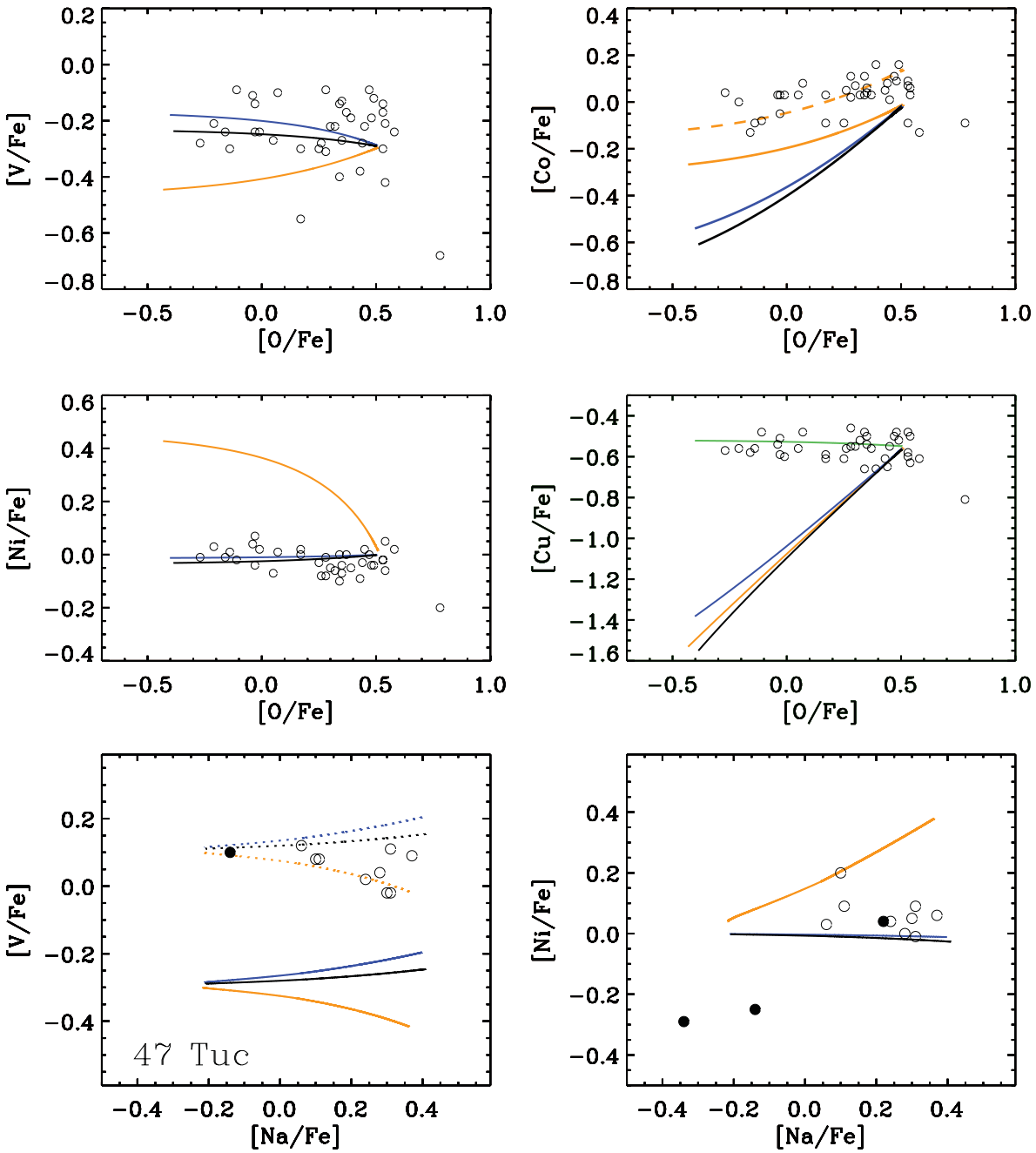

Figure 9. Upper four panels: evolution of Fe-group elements ([V/Fe], [Co/Fe], [Ni/Fe] and [Cu/Fe]) versus [O/Fe] for the case of NGC 6752; open symbols correspond to the observational data from Yong et al. (2005). Bottom two panels: evolution of Fe-group elements ([V/Fe] and [Ni/Fe]) versus [Na/Fe] for the case of 47 Tuc; open symbols correspond to the observational data from Carretta et al. (2005). In all six panels, the colour-coded lines refer to models with different SNe Ia yields. Orange lines: W7; blue lines: WDD1; black lines: CDD1. Dashed lines in the upper right-hand and bottom left-hand panels correspond to the arbitrary ∼0.1–0.3 dex model offsets required to match the extant data (see text for details). The green line in the middle right-hand panel corresponds to a model in which the Cu production in SNe Ia is assumed to be $\sim 1.2 \times 10^{-4}$ $M_{\odot}$, in order to match the observational constraints.

As already noted by Iwamoto et al. (1999), even if different SN Ia models can produce slightly different yields, they all agree that an SN Ia should produce heavy neutron-rich isotopes, such as ^{50}Ti, ^{58}Fe and ^{58}Ni. In Table 4 we summarize the isotope ratios of these elements for different SNe II and SNe Ia models in the literature. For the following, the SNe II yields we use are labelled 'SNe II model' in Table 4, while we will test the different ratios associated with different yields for SNe Ia.

In Fig. 10, we show the predictions of our NGC 6752 and 47 Tuc models for the evolution of the isotope ratios ^{48}Ti/^{50}Ti, ^{56}Fe/^{58}Fe and ^{58}Ni/^{60}Ni versus [O/Fe]. As can be seen, variations of up to two orders of magnitude are predicted and should be observed if inhomogeneous pollution by the SN Ia is the condition for a GC's formation. Indeed, as ^{50}Ti and ^{58}Fe are primarily produced in SN Ia, and marginally produced in SNe II, the ^{56}Fe/^{58}Fe and ^{48}Ti/^{50}Ti isotope ratios increase considerably during the formation of the GC.

Table 4. Isotope ratios for the averaged yields of SNe II and SNe Ia. The labels are the same as used in Tables 1 and 2.

	^{48}Ti/^{50}Ti	^{56}Fe/^{58}Fe	^{58}Ni/^{60}Ni
SNe II (W&W)	1.1e–4	3.7e–4	0.5
SNe II (KOB)	2.3e–2	1.7e–3	0.36
SNe II (C&L)	0.9e–4	6.6e–4	2.0
Model (SNe II)	1.e–4	5.e–4	0.5
SNe Ia (W7)	1.9	2.1e–2	8.8
SNe Ia (WDD1)	2.0	1.8e–2	6.2
SNe Ia (WDD3)	35.2	6.5e–2	11.2

The case of ^{58}Ni and ^{60}Ni is slightly different since both isotopes are produced by both types of SNe. In this case, the ^{58}Ni production by SN Ia should be observable even if there is *only* a change of 0.8–1.0 dex in the ^{58}Ni/^{60}Ni ratio, which decreases during the evolution.

While the measurements of such isotope ratios would help to test our framework, from an observational perspective such measurements are likely beyond the limit of current instrumentation. It might be possible to measure Fe isotope ratios from the Fe–H molecular lines; such lines are most likely to be present in extremely cool dwarfs. This is beyond the observational capabilities of current instrumentation but it might be possible using projected high-resolution near-infrared spectrographs on 40-m class telescopes. Isotope ratios for Ti have been measured in only a handful of near-solar metallicity stars (e.g. Lambert & Luck 1977; Chavez & Lambert 2009). These isotopes can only be measured from TiO molecular lines, and such lines are only present in metal-rich giants ([Fe/H] ≥ -0.7) or very cool dwarfs. Since NGC 6752 is reasonably metal-poor, the only possibility of finding TiO lines would be at the very cool end of the main sequence, beyond current instrumentation. Owing to its higher metallicity, 47 Tuc ([Fe/H] ~ 0.7) may be an excellent candidate to test our predictions with current capabilities while measurements in other more metal-poor GCs will be possible with the advent of the 40-m class telescopes.

As shown by Hughes et al. (2008), the Chavez & Lambert (2009) data suggest that mildly subsolar metallicity giants in the disc+halo show $\log(^{48}\mathrm{Ti}/^{50}\mathrm{Ti}) \approx 1.1$, with very little variation from [Fe/H] ≈ -0.7 to [Fe/H] $\approx +0.0$. If confirmed in a metal-rich GC like 47 Tuc, this would suggest that the W7 or WDD1 SNe Ia models are to be preferred over the CDD1 model (which is $\sim$0.7 dex higher in $\log(^{48}\mathrm{Ti}/^{50}\mathrm{Ti})$ in this metallicity range).

8 CONCLUSIONS

In this paper, we continue the study of the chemical evolution of GCs in the new framework of 'peculiar pre-enrichment' presented by Marcolini et al. (2008). We extend the previous study to the very metal-poor globular clusters M15 and NGC 6397 and the metal-rich cluster 47 Tuc. We also study the chemical evolution of fluorine in M4. Our major findings can be summarized as follows.

(i) In our framework we can reproduce the sodium–fluorine anti-correlation, as well as the oxygen–fluorine correlation observed in M4.

(ii) The model can reproduce the very low [Fe/H] contents of M15 and NGC 6397 assuming that they formed early in the history of the halo, and that the SN Ia+AGB stars' inhomogeneous pollution was localized in a larger radius (compared to the more

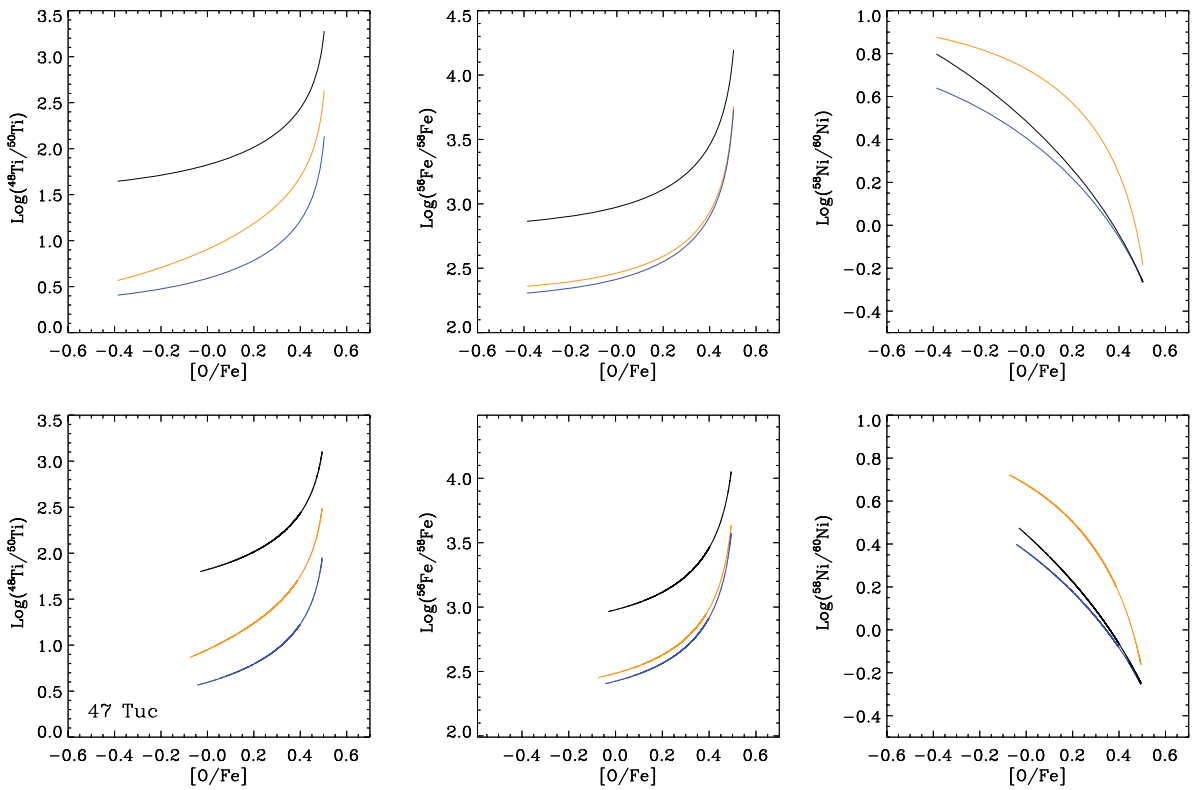

Figure 10. Evolution of the isotope ratios for ^{48}Ti/^{50}Ti, ^{56}Fe/^{58}Fe and ^{58}Ni/^{60}Ni versus [O/Fe], for the NGC 6752 model (upper panels) and for 47 Tuc (lower panels). The isotopes ^{50}Ti, ^{58}Fe and ^{58}Ni are mainly produced by SNe Ia (Iwamoto et al. 1999). The colour-coded lines correspond to models with different SNe Ia yields. Orange lines: W7; blue lines: WDD1; black lines: CDD1.

metal-rich clusters). The Na–O and C–N anti-correlations are also well reproduced for these cases.

(iii) The light-element anti-correlations are also reproduced in the case of the metal-rich globular cluster 47 Tuc, which in our framework should form at a later stage of the halo's formation, with the inhomogeneous pollution confined to a much smaller radius (e.g. $\sim$20 pc).

(iv) We also tested our model against the observed α-element abundances (O, Mg, Si, Ca and Ti) for different SNe Ia models. In general, the slow deflagration SN Ia models (WDD1 and CDD1) of Iwamoto et al. (1999) better reproduce the observational constraints than the fast deflagration (W7) models. This is because the WDD1 and CDD1 models produce more Si, Ca and Ti. The model reproduces the α-element content in the case of the metal-rich globular 47 Tuc, where a slight Na–Si and Na–Ca anti-correlation is observed. In the case of the intermediate-metallicity globular NGC 6752, we predict a moderate Si–O and Ca–O correlation which is not compatible with observations. However, this problem can be solved by assuming that (very) low metallicity (or prompt) SNe Ia produce a factor of 2 (2) more Si (Ca) than the yields prescribed by Iwamoto et al. (1999), which were computed for solar metallicity. Also, more Si production by intermediate-mass AGB stars would also help to solve this problem. This last point, though, is not compatible with current AGB models.

(v) The model predicts that the evolution of most of the Fe-peak elements should remain approximately constant (V and Ni) or slightly anti-correlated with oxygen (Co). This is because SNe Ia yields prescribe a large production of the Fe-group elements (with the slow deflagration model better fitting the observations). However, while our model in general predicts that Fe-group elements should slightly correlate or anti-correlate with lighter elements, the details (and the scatter) depend strongly on the adopted SNe II yields, with yields at different metallicities required (especially for SNe Ia) for a more detailed analysis.

(vi) The only notable exception is copper, which we fail to reproduce by more than an order of magnitude when using yields from the literature. This is due to the low Cu production in theoretical SNe Ia models. We propose a value for the copper production of $\sim 1.2 \times 10^{-4}$ M$_\odot$ in SNe Ia, to match the observational constraints. While copper production is still a matter of debate in the literature, it is worth noting that our proposed value is essentially the same as suggested by Matteucci et al. (1993), to reproduce the copper abundances of the disk+halo of the Milky Way.

(vii) Finally, we propose that the discovery of high isotopic ratios (at high [α/Fe]) involving the neutron-rich ^{50}Ti, ^{58}Fe and ^{58}Ni species could be used as an observational test of our model. This is because these are mainly produced by SN Ia, unlike the Mg isotopes employed in Paper I which are produced by both SNe II and AGB stars. This test will likely only be possible for the most metal-rich clusters such as 47 Tuc.

(viii) The dynamical feasibility of the proposed scenario, however, remains to be probed with hydrodynamical simulations.

ACKNOWLEDGMENTS

We kindly thank David Yong for his insights into isotopic abundance determinations. PSB is supported by the Ministerio de Ciencia e Innovación (MICINN) of Spain through the Ramon y Cajal programme. PSB also acknowledges a Marie Curie Intra-European Reintegration grant within the sixth European framework programme *and* financial support from the Spanish Plan Nacional del Espacio del Ministerio de Educación y Ciencia (AYA2007-67752-C03-01). BKG acknowledges support of the UK's Science and Technology Facilities Council (STFC: ST/F002432/1 and ST/G003025/1), the UK's National Cosmology Supercomputer (COSMOS), the University of Central Lancashire's High Performance Computing Facility, and the generous financial support of St Mary's and Monash Universities visitor programmes. AIK acknowledges support from the Australian Research Council's Discovery Projects funding scheme (DP0664105).

REFERENCES

Alves-Brito A. et al., 2005, A&A, 435, 657
Bekki K., 2010, ApJ, 724, L99
Bekki K., Norris J. E., 2006, ApJ, 637, 109
Bekki K., Campbell S. W., Lattanzio J. C., Norris J. E., 2007, MNRAS, 377, 335
Bonifacio P. et al., 2007, A&A, 470, 153
Briley M. M., Harbeck D., Smith G. H., Grebel E. K., 2004, AJ, 127, 1588
Carretta E., Gratton R. G., Bragaglia A., Bonifacio P., Pasquini L., 2004, A&A, 416, 925
Carretta E., Gratton R. G., Lucatello S., Bragaglia A., Bonifacio P., 2005, A&A, 433, 597
Carretta E., Bragaglia A., Gratton R. G., Leone F., Recio-Blanco A., Lucatello S., 2006, A&A, 450, 523
Charbonnel C., 1994, A&A, 282, 811
Charbonnel C., 1995, ApJ, 453, L41
Chavez J., Lambert D. L., 2009, ApJ, 699, 1906
Chieffi A., Limongi M., 2004, ApJ, 608, 405
Cohen J. G., Meléndez J., 2005, AJ, 129, 303
Cohen J. G., Briley M. M., Stetson P. B., 2002, AJ, 123, 2525
Cottrell P. L., Da Costa G. S., 1981, ApJ, 245, L79
D'Antona F., Caloi V., 2004, ApJ, 611, 871
D'Antona F., Ventura P., 2007, MNRAS, 379, 1431
D'Antona F., Bellazzini M., Caloi V., Pecci F. F., Galleti S., Rood R. T., 2005, ApJ, 631, 868
D'Ercole A., Vesperini E., D'Antona F., McMillan S. L. W., Recchi S., 2008, MNRAS, 391, 825
Dantona F., Gratton R., Chieffi A., 1983, Mem. Soc. Astron. Ital., 54, 173
de Silva G. M., Gibson B. K., Lattanzio J., Asplund M., 2009, A&A, 500, L25
Decressin T., Charbonnel C., Meynet G., 2007a, A&A, 475, 859
Decressin T., Meynet G., Charbonnel C., Prantzos N., Ekström S., 2007b, A&A, 464, 1029
Denissenkov P. A., Herwig F., 2003, ApJ, 590, L99
Denissenkov P. A., Tout C. A., 2000, MNRAS, 316, 395
Fenner Y., Gibson B. K., Lee H., Karakas A. I., Lattanzio J. C., Chieffi A., Limongi M., Yong D., 2003, Proc. Astr. Soc. Aust., 20, 340
Fenner Y., Campbell S., Karakas A. I., Lattanzio J. C., Gibson B. K., 2004, MNRAS, 353, 789
Frebel A., Norris J. E., Aoki W., Honda S., Bessell M. S., Takada Hidai M., Beers T. C., Christlieb N., 2007, ApJ, 658, 534
Gibson B. K., 1994, J. R. Astron. Soc. Can., 88, 383
Gratton R. G., Sneden C., Carretta E., Bragaglia A., 2000, A&A, 354, 169
Gratton R., Sneden C., Carretta E., 2004, ARA&A, 42, 385
Gratton R. G. et al., 2007, A&A, 464, 953
Grundahl F., Briley M., Nissen P. E., Feltzing S., 2002, A&A, 385, L14
Harris W. E., 1996, AJ, 112, 1487
Hughes G. L., Gibson B. K., Carigi L., Sánchez-Blázquez P., Chavez J. M., Lambert D. L., 2008, MNRAS, 390, 1710
Ivans I. I., Sneden C., Kraft R. P., Suntzeff N. B., Smith V. V., Langer G. E., Fulbright J. P., 1999, AJ, 118, 1273
Ivans I. I., Kraft R. P., Sneden C., Smith G. H., Rich R. M., Shetrone M., 2001, AJ, 122, 1438
Iwamoto K., Brachwitz F., Nomoto K., Kishimoto N., Umeda H., Hix W. R., Thielemann F.-K., 1999, ApJS, 125, 439
Jehin E., Magain P., Neuforge C., Noels A., Thoul A. A., 1998, A&A, 330, L33

Karakas A. I., Lattanzio J. C., 2003, Proc. Astr. Soc. Aust., 20, 279
Karakas A., Lattanzio J. C., 2007, Proc. Astr. Soc. Aust., 24, 103
Karakas A. I., Lee H. Y., Lugaro M., Görres J., Wiescher M., 2008, ApJ, 676, 1254
Kobayashi C., Umeda H., Nomoto K., Tominaga N., Ohkubo T., 2006, ApJ, 653, 1145
Koch A., McWilliam A., 2008, AJ, 135, 1551
Kraft R. P., Sneden C., Langer G. E., Shetrone M. D., 1993, AJ, 106, 1490
Lambert D. L., Luck R. E., 1977, ApJ, 211, 443
Mannucci F., Della Valle M., Panagia N., 2006, MNRAS, 370, 773
Marcolini A., D'Ercole A., Battaglia G., Gibson B. K., 2008, MNRAS, 386, 2173
Marcolini A., Gibson B. K., Karakas A. I., Sánchez-Blázquez P., 2009, MNRAS, 395, 719
Marino A. F., Villanova S., Piotto G., Milone A. P., Momany Y., Bedin L. R., Medling A. M., 2008, A&A, 490, 625
Matteucci F., Recchi S., 2001, ApJ, 558, 351
Matteucci F., Raiteri C. M., Busson M., Gallino R., Gratton R., 1993, A&A, 272, 421
Mishenina T. V., Kovtyukh V. V., Soubiran C., Travaglio C., Busso M., 2002, A&A, 396, 189
Parmentier G., Jehin E., Magain P., Neuforge C., Noels A., Thoul A. A., 1999, A&A, 352, 138
Pasquini L., Bonifacio P., Molaro P., Francois P., Spite F., Gratton R. G., Carretta E., Wolff B., 2005, A&A, 441, 549
Prantzos N., Charbonnel C., 2006, A&A, 458, 135
Ramírez S. V., Cohen J. G., 2003, AJ, 125, 224
Romano D., Matteucci F., 2007, MNRAS, 378, L59
Ryan S. G., Norris J. E., 1991, AJ, 101, 1865
Salpeter E. E., 1955, ApJ, 121, 161
Schaller G., Schaerer D., Meynet G., Maeder A., 1992, A&AS, 96, 269
Smith G. H., 1987, PASP, 99, 67
Smith G. H., Norris J., 1982, ApJ, 254, 594
Smith G. H., Tout C. A., 1992, MNRAS, 256, 449
Smith V. V., Cunha K., Ivans I. I., Lattanzio J. C., Campbell S., Hinkle K. H., 2005, ApJ, 633, 392
Sneden C., Kraft R. P., Shetrone M. D., Smith G. H., Langer G. E., Prosser C. F., 1997, AJ, 114, 1964
Sneden C., Kraft R. P., Guhathakurta P., Peterson R. C., Fulbright J. P., 2004, AJ, 127, 2162
Timmes F. X., Woosley S. E., Weaver T. A., 1995, ApJS, 98, 617
Tsujimoto T., Shigeyama T., Suda T., 2007, ApJ, 654, L139
Weiss A., Denissenkov P. A., Charbonnel C., 2000, A&A, 356, 181
Woosley S. E., Weaver T. A., 1995, ApJS, 101, 181
Yong D., Grundahl F., Lambert D. L., Nissen P. E., Shetrone M. D., 2003, A&A, 402, 985
Yong D., Grundahl F., Nissen P. E., Jensen H. R., Lambert D. L., 2005, A&A, 438, 875
Yong D., Grundahl F., Johnson J. A., Asplund M., 2008, ApJ, 684, 1159

This paper has been typeset from a TEX/LATEX file prepared by the author.